

Constraining Nonstandard Neutrino-Electron Interactions

J. Barranco,^{*} O. G. Miranda,[†] and C. A. Moura[‡]

*Departamento de Física, Centro de Investigación y de Estudios Avanzados del IPN,
Apdo. Postal 14-740 07000 México, D.F., Mexico*

J.W.F.Valle[§]

*AHEP Group, Instituto de Física Corpuscular – C.S.I.C./Universitat de València
Edificio Institutos de Paterna, Apt 22085, E-46071 Valencia, Spain*

Abstract

We present a detailed analysis on non-standard neutrino interactions (NSI) with electrons including all muon and electron (anti)-neutrino data from existing accelerators and reactors, in conjunction with the “neutrino counting” data ($e^+e^- \rightarrow \nu\bar{\nu}\gamma$) from the four LEP collaborations. First we perform a one-parameter-at-a-time analysis, showing how most constraints improve with respect to previous results reported in the literature. We also present more robust results where the NSI parameters are allowed to vary freely in the analysis. We show the importance of combining LEP data with the other experiments in removing degeneracies in the global analysis constraining flavor-conserving NSI parameters which, at 90% and 95% C.L., must lie within unique allowed regions. Despite such improved constraints, there is still substantial room for improvement, posing a big challenge for upcoming experiments.

^{*}Electronic address: jbarranc@fis.cinvestav.mx; Present address: Instituto de Física, Universidad Nacional Autónoma de México, Apdo. Postal 20-364, 01000 México D.F., Mexico

[†]Electronic address: Omar.Miranda@fis.cinvestav.mx

[‡]Electronic address: cadrega@fis.cinvestav.mx; On leave from: Instituto de Física Gleb Wataghin - UNICAMP, Brazil

[§]Electronic address: valle@ific.uv.es

I. INTRODUCTION

The historic discovery of neutrino oscillations constitutes the first evidence for physics beyond the Standard Model, and one would like to know to which direction it is pointing. Despite a pretty good knowledge of the neutrino oscillation mechanism and the parameters involved [1], the nature of the mechanism generating masses and mixings remains as elusive as ever. Neutrino mass models fall in various classes [2] involving models where neutrinos get mass *a la seesaw* [3, 4, 5, 6, 7, 8, 9], those where neutrinos acquire mass radiatively due to the presence of extra Higgs bosons [10, 11, 12], and hybrid models, like those based on low energy supersymmetry with spontaneous (or bilinear) breaking of R-parity [13, 14, 15, 16, 17]. Starting with the seesaw [7] all those mechanisms carry with them modifications to the structure of the standard electroweak neutral and charged currents. The simplest of such modifications in the low energy regime may be written in the usual $V - A$ form, similar to the four-Fermi interaction, characterized by some new coupling, which we generally call, in what follows, Non-Standard Interactions (NSI). Such interactions can arise in a variety of ways, e. g., from the exchange of Higgs and/or supersymmetric scalar bosons as well as a new heavy gauge boson, such as a Z' . Non-standard interactions can conserve flavor, their differences characterizing the violation of weak universality, known as Non-Universal (NU) NSI. Alternatively, they may violate flavor conservation, known as Flavor Changing (FC) NSI.

On the other hand, current neutrino oscillation data, as inferred from the solar [18, 19, 20] and atmospheric [21, 22, 23] neutrino experiments, leave significant room for the existence of sub-leading effects induced by NSI. In fact, NSI effects may be comparable to oscillation effects in solar neutrino physics, where indeed a new degenerate solution is still allowed [18]. At this stage laboratory experiments both from accelerators and reactors can play a crucial role, since the strongest sensitivity to NSI comes from this kind of experiments [24]. Precision measurements of oscillation parameters in long baseline oscillation experiments such as neutrino factories will also benefit from improved NSI studies. These could help resolving the confusion between the two found in Refs. [25, 26] and further discussed in Refs. [27, 28].

Here we address the current sensitivity on non-standard interactions as inferred from a global analysis of processes involving (anti)-neutrinos and electrons. Previous analyses have been performed in Refs. [24, 29, 30, 31]. Our current analysis combines the relevant experimental “neutrino counting” data from $e^+ + e^- \rightarrow \nu + \bar{\nu} + \gamma$ obtained by the four LEP collaborations [32, 33, 34, 35, 36, 37, 38, 39, 40, 41], and summarized in Ref. [42], with all the $\nu_e + e \rightarrow \nu_e + e$ data obtained by LSND [43], and the $\bar{\nu}_e + e \rightarrow \bar{\nu}_e + e$ interaction studied in reactor experiments, namely: Irvine [44], MUNU [45] and Rovno [46]. For the muon

neutrino case the relevant reactions are $\nu_\mu + e \rightarrow \nu_\mu + e$ and $\bar{\nu}_\mu + e \rightarrow \bar{\nu}_\mu + e$, measured at CHARM II [47]. Our analysis is also novel in the sense that we adopt a model independent approach, as general as possible, allowing simultaneous variations of all NSI parameters. In particular, we compare the restrictions obtained varying only one parameter at a time, with those obtained in the case where all six flavor-conserving parameters are left free.

The analysis sketched above is organized as follows: in Sec. II the NSI are introduced and the relevant cross sections are expressed as function of NSI parameters, in Secs. III and IV we briefly present the data and the details of the χ^2 analysis. The results are presented in Sec. V and more discussion and outlook are given in Sec. VI.

II. NON-STANDARD INTERACTIONS AND RELEVANT CROSS SECTIONS

Neutrino NSI constitute an unavoidable characteristic feature of gauge models of neutrino mass, for example those where they arise from the admixture of isodoublet and isosinglet neutral leptons, like models of the generic seesaw type [7]. Typically the masses of the light neutrinos are obtained by diagonalizing the mass matrix

$$\begin{bmatrix} M_L & D \\ D^T & M_R \end{bmatrix} \quad (1)$$

in the basis ν, ν^c , where D is the standard $SU(2) \otimes U(1)$ breaking Dirac mass term, and $M_R = M_R^T$ is the large isosinglet Majorana mass. In the absence of the isotriplet (type-II) $M_L \nu \nu$ term [7] the scheme is called type-I seesaw [3, 4, 5, 6]. In models with spontaneous breaking of lepton number symmetry one has $M_L \propto 1/M_R$, a feature that comes from the study of the scalar potential and holds both in the case of left-right models (gauged lepton number) [9] and the case of majoron models (ungauged lepton number) [8].

The structure of the associated effective $SU(2) \otimes U(1)$ weak $V - A$ currents is rather complex and deviates from standard [7]. The first point to notice is that the heavy isosinglets will mix with the ordinary isodoublet neutrinos in the charged current weak interaction. As a result, the mixing matrix describing the charged leptonic weak interaction is a rectangular matrix K [7] which may be decomposed as

$$K = (K_L, K_H) \quad (2)$$

where K_L and K_H are 3×3 matrices. Note that the ‘‘effective’’ lepton mixing matrix K_L relevant in oscillation studies is non-unitary [50]. For papers addressing possible future tests of such non-unitary effects see for example [51] and references therein. The corresponding

neutral weak interactions are described by a non-trivial matrix [7] $K^\dagger K$

$$\mathcal{L} = \frac{ig'}{2\sin\theta_W} Z_\mu \bar{\nu}_L \gamma_\mu K^\dagger K \nu_L. \quad (3)$$

Such structure of the charged and neutral weak currents provides an origin for neutrino NSI. Note, however, that the smallness of neutrino mass, which follows due to the seesaw mechanism $M_{\nu\text{eff}} = M_L - DM_R^{-1}D^T$ and the condition $M_L \ll M_R$, implies that, barring fine-tuning, the magnitude of neutrino NSI and its effects are expected to be negligible.

However this need not be so in general. Since the number m of $SU(2) \otimes U(1)$ singlets is arbitrary, one may, for example, extend the lepton sector of the $SU(2) \otimes U(1)$ theory by adding a set of *two* 2-component isosinglet neutral fermions, denoted ν^c_i and S_i , in each generation. In such $m = 6$ models one can consider the 9×9 mass matrix [48, 49]

$$\begin{bmatrix} 0 & D & 0 \\ D^T & 0 & M \\ 0 & M^T & \mu \end{bmatrix} \quad (4)$$

(in the basis ν, ν^c, S). The Majorana masses for the neutrinos are determined from

$$M_L = DM^{-1}\mu M^T D^T. \quad (5)$$

Since in the limit $\mu \rightarrow 0$ the exact lepton number symmetry is recovered and neutrinos become massless [48] this scheme is sometimes called ‘‘inverse seesaw’’ [66].

This provides an elegant way to generate neutrino masses without a super-heavy scale, the smallness of the neutrino mass indicated by the oscillation interpretation of solar and atmospheric neutrino data is ascribed to the smallness of μ , which is natural in ‘t Hooft’s sense: the symmetry of the theory is enhanced in the limit of vanishing μ . This automatically allows for a sizeable magnitude of neutrino NSI strengths, unconstrained by the smallness of neutrino masses [67].

The NSI which are engendered in this case will necessarily affect neutrino propagation properties in matter, an effect that may be resonant in certain cases [50, 52, 53]. They may also be large enough as to produce effects in the laboratory.

An alternative way to induce neutrino NSI is in the context of low-energy supersymmetry without R-parity conservation [54, 55, 56] where one may also have, in addition to bilinear [13, 14, 15, 16] also trilinear L violating couplings in the super-potential such as

$$\lambda_{ijk} L_i L_j E_k^c \quad (6)$$

$$\lambda'_{ijk} L_i Q_j D_k^c \quad (7)$$

where L, Q, E^c and D^c are (chiral) super-fields which contain the usual lepton and quark $SU(2)$ doublets and singlets, respectively, and i, j, k are generation indices. The couplings in Eq. (6) give rise at low energy to the following four-fermion effective Lagrangian for neutrino interactions with d -quark including

$$\mathcal{L}_{\text{eff}} = -2\sqrt{2}G_F \sum_{\alpha,\beta} \xi_{\alpha\beta} \bar{\nu}_{L\alpha} \gamma^\mu \nu_{L\beta} \bar{d}_R \gamma^\mu d_R \quad \alpha, \beta = e, \mu, \tau, \quad (8)$$

where the parameters $\xi_{\alpha\beta}$ represent the strength of the effective interactions normalized to the Fermi constant G_F . One can identify explicitly, for example, the following *non-standard* flavor-conserving NSI couplings

$$\xi_{\mu\mu} = \sum_j \frac{|\lambda'_{2j1}|^2}{4\sqrt{2}G_F m_{\tilde{q}_{jL}}^2}, \quad (9)$$

$$\xi_{\tau\tau} = \sum_j \frac{|\lambda'_{3j1}|^2}{4\sqrt{2}G_F m_{\tilde{q}_{jL}}^2}, \quad (10)$$

and the FC coupling

$$\xi_{\mu\tau} = \sum_j \frac{\lambda'_{3j1} \lambda'_{2j1}}{4\sqrt{2}G_F m_{\tilde{q}_{jL}}^2} \quad (11)$$

where $m_{\tilde{q}_{jL}}$ are the masses of the exchanged squarks and $j = 1, 2, 3$ denotes $\tilde{d}_L, \tilde{s}_L, \tilde{b}_L$, respectively. The existence of effective neutral current interactions contributing to the neutrino scattering off d -quarks in matter, provides new flavor-conserving as well as flavor-changing terms for the matter potentials of neutrinos. Such NSI are directly relevant for solar [18, 19, 20] and atmospheric neutrino propagation [21, 22, 23].

In what follows we consider a more general class of non-standard interactions described via the effective four fermion Lagrangian,

$$- \mathcal{L}_{\text{NSI}}^{eff} = \varepsilon_{\alpha\beta}^{fP} 2\sqrt{2}G_F (\bar{\nu}_\alpha \gamma_\rho L \nu_\beta) (\bar{f} \gamma^\rho P f), \quad (12)$$

where G_F is the Fermi constant and $\varepsilon_{\alpha\beta}^{fP}$ parametrize the strength of the NSI. For laboratory experiments f is a first generation SM fermion (e, u or d). Here we analyze only processes involving electrons, so that in what follows we have only $f = e$. The chiral projectors P denote $\{L, R = (1 \pm \gamma^5)/2\}$, while α and β denote the three neutrino flavors: e, μ and τ .

In total there are 12 relevant parameters given by $\varepsilon_{\alpha\beta}^P$. In order to constrain these we use experimental data reported by LEP ($e^+e^- \rightarrow \nu\bar{\nu}\gamma$), LSND ($\nu_e e \rightarrow \nu_e e$), CHARM II ($\nu_\mu e$ or $\bar{\nu}_\mu e$ scattering) and reactor experiments ($\bar{\nu}_e e \rightarrow \bar{\nu}_e e$). The cross sections for the interactions of each experiment are given next.

A. LEP cross section

The $e^+e^- \rightarrow \nu\bar{\nu}\gamma$ cross section can be calculated at tree level using the ‘radiator’ approximation to describe the photon emission [57] as

$$\sigma_{\text{LEP}}^{\text{theo}}(s) = \int dx \int dc_\gamma H(x, s_\gamma; s) \sigma_0^{\text{theo}}(\hat{s}), \quad (13)$$

where s is the center of mass energy, $x = 2E_\gamma/\sqrt{2}$, E_γ is the photon energy, $\sigma_0^{\text{theo}} = \sigma_0^{\text{SM}} + \sigma_0^{\text{NSI}}$ is the cross section for the process $e^+e^- \rightarrow \nu\bar{\nu}$ and $\hat{s} = (1-x)s$. Here the ‘radiator’ function H is given by

$$H(x, s_\gamma; s) = \frac{2\alpha}{\pi x s_\gamma} \left[\left(1 - \frac{x}{2}\right)^2 + \frac{x^2 c_\gamma^2}{4} \right], \quad (14)$$

where $s_\gamma \equiv \sin \theta_\gamma$ and $c_\gamma^2 \equiv 1 - s_\gamma^2$, with θ_γ being the photon emission angle.

Working in the limit of vanishing $W-\gamma$ interactions but considering finite distance effects for the W propagator, the Standard Model $e^+e^- \rightarrow \nu\bar{\nu}$ cross section is given as

$$\begin{aligned} \sigma_0^{\text{SM}}(s) &= \frac{N_\nu G_F^2}{6\pi} M_Z^4 (g_R^2 + g_L^2) \frac{s}{[(s - M_Z^2)^2 + (M_Z \Gamma_Z)^2]} \\ &+ \frac{G_F^2}{\pi} M_W^2 \left\{ \frac{s + 2M_W^2}{2s} - \frac{M_W^2}{s} \left(\frac{s + M_W^2}{s} \right) \log \left(\frac{s + M_W^2}{M_W^2} \right) \right. \\ &\left. - g_L \frac{M_Z^2 (s - M_Z^2)}{(s - M_Z^2)^2 + (M_Z \Gamma_Z)^2} \left[\frac{(s + M_W^2)^2}{s^2} \log \left(\frac{s + M_W^2}{M_W^2} \right) - \frac{M_W^2}{s} - \frac{3}{2} \right] \right\}, \end{aligned} \quad (15)$$

where N_ν is the number of neutrino families, g_R and g_L are the SM electron coupling constants to the Z -boson, M_W , M_Z and Γ_Z are the W and Z -boson masses, and total Z decay width respectively.

The NU and FC components of the nonstandard cross section, $\sigma_0^{\text{NSI}} = \sigma_0^{\text{NU}} + \sigma_0^{\text{FC}}$, are given by [29]:

$$\begin{aligned} \sigma_0^{\text{NU}}(s) &= \sum_{\alpha=e,\mu,\tau} \frac{G_F^2}{6\pi} s \left[(\varepsilon_{\alpha\alpha}^L)^2 + (\varepsilon_{\alpha\alpha}^R)^2 - 2(g_L \varepsilon_{\alpha\alpha}^L + g_R \varepsilon_{\alpha\alpha}^R) \frac{M_Z^2 (s - M_Z^2)}{(s - M_Z^2)^2 + (M_Z \Gamma_Z)^2} \right] \\ &+ \frac{G_F^2}{\pi} \varepsilon_{ee}^L M_W^2 \left[\frac{(s + M_W^2)^2}{s^2} \log \left(\frac{s + M_W^2}{M_W^2} \right) - \frac{M_W^2}{s} - \frac{3}{2} \right], \end{aligned} \quad (16)$$

$$\sigma_0^{\text{FC}}(s) = \sum_{\alpha \neq \beta = e,\mu,\tau} \frac{G_F^2}{6\pi} s [(\varepsilon_{\alpha\beta}^L)^2 + (\varepsilon_{\alpha\beta}^R)^2]. \quad (17)$$

B. LSND and reactors cross sections

The differential cross section for $\nu_e e$ scattering processes in the presence of NSI can be written as

$$\begin{aligned} \frac{d\sigma_{\text{LSND}}^{\text{theo}}}{dT} &= \frac{2G_F^2 m_e}{\pi} [(\tilde{g}_L^2 + \sum_{\alpha \neq e} |\varepsilon_{\alpha e}^L|^2) + \\ &+ (\tilde{g}_R^2 + \sum_{\alpha \neq e} |\varepsilon_{\alpha e}^R|^2) \left(1 - \frac{T}{E_\nu}\right)^2 - (\tilde{g}_L \tilde{g}_R + \sum_{\alpha \neq e} |\varepsilon_{\alpha e}^L| |\varepsilon_{\alpha e}^R|) m_e \frac{T}{E_\nu^2}], \end{aligned} \quad (18)$$

where T is the electron recoil energy, m_e is the electron mass and E_ν is the incident neutrino energy. The effective couplings $\tilde{g}_{R,L}$ are given as $\tilde{g}_R = g_R + \varepsilon_{ee}^R$ and $\tilde{g}_L = g_L + \varepsilon_{ee}^L$. For the case of reactors, we have to exchange L by R and vice-versa.

C. CHARM II cross section

In the presence of NSI the differential $\nu_\mu e \rightarrow \nu_\alpha e$ cross section relevant for the case of the CHARM II experiment is given as

$$\frac{d\sigma_{\text{CHARM}}^{\text{theo}}}{dy} = \frac{2G_F^2 m_e}{\pi} E_\nu \left[\left(\tilde{g}_L^2 + \sum_{\alpha \neq \mu} |\varepsilon_{\alpha \mu}^L|^2 \right) + \left(\tilde{g}_R^2 + \sum_{\alpha \neq \mu} |\varepsilon_{\alpha \mu}^R|^2 \right) (1 - y)^2 \right] \quad (19)$$

where $\tilde{g}_{L,R} = g_{L,R} + \varepsilon_{\mu\mu}^{L,R}$ and $y = (1 - \cos\theta^*)/2$ is called the inelasticity. Here θ^* is the center of mass scattering angle. For the anti-neutrino case, we simply have to exchange L by R and vice-versa.

III. THE DATA

In what follows we will mainly focus on the effect of the six flavor conserving non-standard interactions in the above processes. Generalizing to include also the six flavor changing NSI parameters is straightforward but technically more complex and somewhat less motivated in view of strong, albeit indirect, bounds that follow from searches for lepton flavor violation. Let us now first briefly describe the relevant data used in our global analysis.

A. The LEP data

Neutrino-electron NSI will contribute to the cross section of the interaction $e^+e^- \rightarrow \nu\bar{\nu}\gamma$ by increasing or decreasing the expected number of events. The best data on such interaction has been collected by the four LEP experiments: OPAL, ALEPH, L3 and DELPHI [32,

33, 34, 35, 36, 37, 38, 39, 40, 41]. The reported measurements are compiled in Table I [42]. The center of mass energy and luminosity for each of the four LEP experiments are given in the second and third columns of Table I. The background subtracted experimental cross sections and the Monte Carlo expectations are given in picobarns in columns four and five respectively. Column six reports the number of events observed after background subtraction. The efficiency ϵ is given in column seven and finally, the last two columns report the kinematical cuts: $x = E_\gamma/E_{beam}$, $x_T = x \sin \theta_\gamma$ with θ_γ the angle between the photon momentum and the beam direction, and $y = \cos \theta_\gamma$. As in [42], we have found that our calculation for the Standard Model LEP cross section, Eq. (13) without including the effects of the NSI, disagrees with the Monte Carlo results quoted by the four collaborations. This might be due to additional specific experimental cuts beside the ones quoted in the last two columns in Table I. Such disagreements are included as an additional theoretical uncertainty which we have added in quadrature in the calculation of our errors.

In total the four LEP experiments lead to 25 observables. Because of the small systematic error they have, we can assume that all of them are independent with no correlation between them.

B. The LSND and reactors data

The best measurements of the cross section for the $\nu_e e$ and $\bar{\nu}_e e$ scattering processes have been performed in terrestrial experiments. The cross section for the elastic scattering interaction $\nu_e + e^- \rightarrow \nu_e + e^-$ was measured by the Liquid Scintillator Neutrino Detector (LSND) using a μ^+ decay-at-rest ν_e beam at the Los Alamos Neutron Science Center. The detector is an approximately cylindrical tank containing 167 tons of liquid scintillator and viewed by 1220 photomultiplier tubes. The final neutrino-electron cross section is reported in Table II [43].

The Irvine [44], the most recent MUNU [45] and the Rovno [46] experiments have measured the $\bar{\nu}_e e$ scattering by using neutrinos from reactors. The measured cross section is also reported in Table II. We also quoted the number of events for each experiment in column three and the recoil electron energy range in column two.

C. The CHARM II data

The CHARM collaboration used a massive 692 ton target calorimeter followed by a muon spectrometer to detect the $\nu_\mu + e \rightarrow \nu_\mu + e$ and $\bar{\nu}_\mu + e \rightarrow \bar{\nu}_\mu + e$ scattering processes. The neutrinos were produced by a 450 GeV proton beam accelerated in the Super Proton

TABLE I: Summary of the ALEPH, DELPHI, L3 and OPAL experimental data, collected above the W^+W^- production threshold. Wherever a double error is listed, the first is statistical and the second is systematic.

	\sqrt{s} (GeV)	\mathcal{L} (pb $^{-1}$)	σ^{mes} (pb)	σ^{MC} (pb)	N_{obs}	ϵ (%)	E_γ (GeV)	$ y $
ALEPH	161	11.1	$5.3 \pm 0.8 \pm 0.2$	5.81 ± 0.03	41	70	$x_T \geq 0.075$	≤ 0.95
[32]	172	10.6	$4.7 \pm 0.8 \pm 0.2$	4.85 ± 0.04	36	72	$x_T \geq 0.075$	≤ 0.95
[33]	183	58.5	$4.32 \pm 0.31 \pm 0.13$	4.15 ± 0.03	195	77	$x_T \geq 0.075$	≤ 0.95
	189	173.6	$3.43 \pm 0.16 \pm 0.06$	3.48 ± 0.05	484			
	192	28.9	$3.47 \pm 0.39 \pm 0.06$	3.23 ± 0.05	81			
	196	79.9	$3.03 \pm 0.22 \pm 0.06$	3.26 ± 0.05	197			
[34]	200	87.0	$3.23 \pm 0.21 \pm 0.06$	3.12 ± 0.05	231	81.5	$x_T \geq 0.075$	≤ 0.95
	202	44.4	$2.99 \pm 0.29 \pm 0.05$	3.07 ± 0.05	110			
	205	79.5	$2.84 \pm 0.21 \pm 0.05$	2.93 ± 0.05	182			
	207	134.3	$2.67 \pm 0.16 \pm 0.05$	2.80 ± 0.05	292			
DELPHI [35]								
HPC	189	154.7	$1.80 \pm 0.15 \pm 0.14$	1.97	146	51 ^a	$x \geq 0.06$	≤ 0.70
FEMC	183	49.2	$2.33 \pm 0.31 \pm 0.18$	2.08	65	54 ^a	$x \geq 0.2$	≥ 0.85
FEMC	189	157.7	$1.89 \pm 0.16 \pm 0.15$	1.94	155	50 ^a	$x \leq 0.9$	≤ 0.98
L3	161	10.7	$6.75 \pm 0.91 \pm 0.18$	6.26 ± 0.12	57	80.5	≥ 10	≤ 0.73
[36]							and	
	172	10.2	$6.12 \pm 0.89 \pm 0.14$	5.61 ± 0.10	49	80.7	$E_T \geq 6$	0.80–0.97
[37]	183	55.3	$5.36 \pm 0.39 \pm 0.10$	5.62 ± 0.10	195	65.4	≥ 5	≤ 0.73
							and	
[38]	189	176.4	$5.25 \pm 0.22 \pm 0.07$	5.29 ± 0.06	572	60.8	$E_T \geq 5$	0.81–0.97
OPAL								
[39]	130	2.3	$10.0 \pm 2.3 \pm 0.4$	13.48 ± 0.22^b	19	81.6	$x_T > 0.05$	≤ 0.82
							or	
	136	2.59	$16.3 \pm 2.8 \pm 0.7$	11.30 ± 0.20^b	34	79.7	$x_T > 0.1$	≤ 0.966
[40]	130	2.35	$11.6 \pm 2.5 \pm 0.4$	14.26 ± 0.06^b	21	77.0		
							$x_T > 0.05$	≤ 0.966
	136	3.37	$14.9 \pm 2.4 \pm 0.5$	11.95 ± 0.07^b	39	77.5		
[39]	161	9.89	$5.3 \pm 0.8 \pm 0.2$	6.49 ± 0.08^b	40	75.2	$x_T > 0.05$	≤ 0.82
							or	
	172	10.28	$5.5 \pm 0.8 \pm 0.2$	5.53 ± 0.08^b	45	77.9	$x_T > 0.1$	≤ 0.966
[40]	183	54.5	$4.71 \pm 0.34 \pm 0.16$	4.98 ± 0.02^b	191	74.2	$x_T > 0.05$	≤ 0.966
[41]	189	177.3	$4.35 \pm 0.17 \pm 0.09$	4.66 ± 0.03	643	82.1	$x_T > 0.05$	≤ 0.966

^aEstimated from the Monte Carlo cross sections and the expected numbers of events.

^bCalculated from the expected number of events as predicted by the KORALZ event generator.

TABLE II: Experimental measurements of the $\nu_e e$ and $\bar{\nu}_e e$ scattering cross sections

Experiment	Energy range (MeV)	Events	Measurement
LSND $\nu_e - e$	10-50	191	$\sigma = [10.1 \pm 1.5] \times E_{\nu_e}(\text{MeV}) \times 10^{-45} \text{cm}^2$
Irvine $\bar{\nu}_e - e$	1.5- 3.0	381	$\sigma = [0.86 \pm 0.25] \times \sigma_{V-A}$
Irvine $\bar{\nu}_e - e$	3.0- 4.5	77	$\sigma = [1.7 \pm 0.44] \times \sigma_{V-A}$
Rovno $\bar{\nu}_e - e$	0.6 - 2.0	41	$\sigma = (1.26 \pm 0.62) \times 10^{-44} \text{cm}^2/\text{fission}$
MUNU $\bar{\nu}_e - e$	0.7 - 2.0	68	$1.07 \pm 0.34 \text{ events day}^{-1}$

Synchrotron (SPS) for 2.5×10^{19} protons on target. Approximately 10^8 neutrino interactions occurred in the detector. Data collected from 1987-1991 were 2677 ± 82 events for reaction $\nu_\mu + e \rightarrow \nu_\mu + e$ and 2752 ± 88 events in the $\bar{\nu}$ beam [47]. There was a neutrino contamination, of approximately 10% of the flux, in the muon-antineutrino electron scattering.

The CHARM collaboration used these data to determine the values of the SM g_A and g_V coupling constants. Because of the quadratic dependence on the coupling constants in the cross section formula given in Eq. (19) there is a well known fourfold ambiguity in the determination of g_V and g_A . A similar ambiguity in determining g_V^e and g_A^e has been removed in [47] by combining the $\nu_e e$ and $\bar{\nu}_e e$ scattering data obtained by the CHARM detector with the forward-backward asymmetry (A_{FB}) in the $e^+e^- \rightarrow e^+e^-$ scattering at LEP [58]. Here we will obtain a similar result in the context of constraining neutrino NSIs but using the ‘‘neutrino counting’’ LEP data.

IV. THE χ^2 ANALYSIS

Once we have defined in the previous sections the cross sections for each of the processes under consideration, and we have introduced all the experimental measurements relevant for our analysis, we proceed to perform a χ^2 analysis.

For the LEP data, we can obtain a theoretical estimate of the expected number of events N_i^{theo} for each of the 25 observables by using Eq. (13). The integration of the cross section has been performed with the experimental cuts reported in last two columns of Table I. We have used the reported luminosity (\mathcal{L}) and efficiency (ϵ) for each experiment.

We define the corresponding χ^2 function as

$$\chi_{\text{LEP}}^2 = \sum_{i=1}^{25} \frac{(N_i^{\text{theo}} - N_i^{\text{obs}})^2}{\Delta_i^2} \quad (20)$$

where N_i^{obs} is reported in Table I and Δ_i is the corresponding error. In the SM limit, our

cross section computations agree within 8% with the LEP Monte Carlo results, except for L3, where we have found up to a 20% discrepancy. Therefore, we have allowed for an extra 10% theoretical systematic error added in quadratures to all LEP experiments [68]. We have neglected all correlations since statistical and systematic errors are small.

For the $\nu_e e$ and $\bar{\nu}_e e$ scattering processes, we define the χ^2 as

$$\chi_{\nu_e e}^2 = \sum_i \frac{(\sigma_i^{\text{theo}} - \sigma_i^{\text{exp}})^2}{\Delta_i^2} \quad (21)$$

where the σ_i^{exp} are given by the experimental measurements and Δ_i are the corresponding errors reported in Table II, while $\sigma_i^{\text{theo}} = \sigma_i^{\text{SM}} + \sigma_i^{\text{NSI}}$ are the theoretical expectations considering the effects of NSI calculated via Eq. (18). Details of the analysis for LSND and reactor experiments constraining NSI in $\nu_e e$ and $\bar{\nu}_e e$ scattering have already been given in Ref. [31].

For CHARM II we calculated the number of events using the cross section from Eq. (19). With the NSI parameters fixed to zero we defined a normalization constant to reproduce the number of events reported by the CHARM II collaboration.

For CHARM II data we have used

$$\chi_{\text{CHARM}}^2 = \sum_{i=1}^2 \frac{(N_i^{\text{theo}} - N_i^{\text{obs}})^2}{\Delta_i^2} \quad (22)$$

where one observable stands for $\nu_\mu e$ scattering and the other one for $\bar{\nu}_\mu e$.

The global χ^2 is simply the sum of the individual ones,

$$\chi_{\text{TOT}}^2 = \chi_{\text{LEP}}^2 + \chi_{\nu_e e}^2 + \chi_{\text{CHARM}}^2. \quad (23)$$

V. RESULTS

The cross section for $e^+ e^- \rightarrow \bar{\nu} \nu \gamma$ including NSI is sensitive to all twelve $\varepsilon_{\alpha\beta}^{L,R}$ parameters. On the one hand the scattering interactions $\nu_e e$ and $\bar{\nu}_e e$ are sensitive to six parameters: $\varepsilon_{e\alpha}^{L,R}$, with $\alpha = e, \mu, \tau$. On the other hand the elastic scatterings $\nu_\mu e$ and $\bar{\nu}_\mu e$ are sensitive to the other six parameters: $\varepsilon_{\mu\alpha}^{L,R}$.

In order to obtain constraints on the relevant NSI parameters, we first follow the most popular approach adopted by the majority of authors [24, 29]. It consists on varying only one parameter at-a-time and fixing the remaining parameters to zero. This way we obtain bounds on the twelve NSI parameters. However such one-parameter-at-a-time analysis is fragile and might miss potential cancellations in the determination of the restrictions upon NSI strengths.

As a second step, we assume that the new physics induces mainly flavor-conserving, effective NU neutral current interactions, so that the only relevant parameters are the six $\varepsilon_{\alpha\alpha}^{L,R}$, $\alpha = e, \mu, \tau$. This is reasonable in view of the relatively strong bounds on lepton flavor violating processes.

A. One parameter at-a-time

In this section we constrain the neutrino-electron NSI parameters varying them one parameter at-a-time. Because each cross section is sensitive to different parameters, depending on the parameter under consideration, the number of total observables used in the analysis will change. Table III shows the χ_{min}^2 , the number of degrees of freedom (d.o.f), the ratio $\chi_{min}^2/\text{d.o.f}$, the allowed range for each of the twelve parameters obtained by our χ^2 analysis and the limits obtained by previous analyses.

TABLE III: Constrains of neutrino-electron NSI parameters by varying only one parameter at-a-time. Improvements are obtained compared with previous analyses. Read text for details.

d.o.f.	χ_{min}^2	$\chi_{min}^2/\text{d.o.f}$	90% C.L. Allowed Region	Previous Limit [24, 31]
29	24.8482	0.8568	$-0.03 < \varepsilon_{ee}^L < 0.08$	$-0.05 < \varepsilon_{ee}^L < 0.1$ ($\nu_e e$)
29	22.4742	0.7750	$0.004 < \varepsilon_{ee}^R < 0.151$	$-0.04 < \varepsilon_{ee}^R < 0.14$ ($\nu_e e$)
26	22.1308	0.8512	$ \varepsilon_{\mu\mu}^L < 0.03$	$ \varepsilon_{\mu\mu}^L < 0.03$ ($\nu_\mu e$)
26	22.1315	0.8512	$ \varepsilon_{\mu\mu}^R < 0.03$	$ \varepsilon_{\mu\mu}^R < 0.03$ ($\nu_\mu e$)
24	21.8927	0.9122	$-0.46 < \varepsilon_{\tau\tau}^L < 0.24$	$-0.6 < \varepsilon_{\tau\tau}^L < 0.4$ ($e^+ e^- \rightarrow \nu\nu\gamma$)
24	21.9072	0.9128	$-0.25 < \varepsilon_{\tau\tau}^R < 0.43$	$-0.4 < \varepsilon_{\tau\tau}^R < 0.6$ ($e^+ e^- \rightarrow \nu\nu\gamma$)
31	22.8752	0.7379	$ \varepsilon_{e\mu}^L < 0.13$	$ \varepsilon_{e\mu}^L \simeq 5 \times 10^{-4}$ ($\mu \rightarrow 3e$)
31	24.9885	0.8061	$ \varepsilon_{e\mu}^R < 0.13$	$ \varepsilon_{e\mu}^R \simeq 5 \times 10^{-4}$ ($\mu \rightarrow 3e$)
29	22.3062	0.7692	$ \varepsilon_{e\tau}^L < 0.33$	$ \varepsilon_{e\tau}^L < 0.4$ ($\nu_e e$)
29	22.2107	0.7659	$0.05 < \varepsilon_{e\tau}^R < 0.28$	$ \varepsilon_{e\tau}^R < 0.27$ ($\nu_e e$)
26	22.1308	0.8512	$ \varepsilon_{\mu\tau}^L < 0.1$	$ \varepsilon_{\mu\tau}^L < 0.1$ ($\nu_\mu e$)
26	22.1312	0.8512	$ \varepsilon_{\mu\tau}^R < 0.1$	$ \varepsilon_{\mu\tau}^R < 0.1$ ($\nu_\mu e$)

One sees how the inclusion of the LEP data leads to an improvement in the constraints for most of the NU NSI parameters. For example, from the last column in Table III one can see how previous constraints on $\varepsilon_{e\alpha}^{L,R}$ coming from LSND and reactor data [24, 31] are now superseded. Our analysis also improves previous constraints on $\varepsilon_{\tau\tau}^{L,R}$. The inclusion of LEP data also improves the limits for $\varepsilon_{e\tau}^{L,R}$. Note that a nonzero $\varepsilon_{e\tau}^R$ is favored in this analysis,

though this has no statistical significance. We can also see that the ratio $\chi_{min}^2/\text{d.o.f.}$ is close to unity in the majority of the cases, meaning that the χ^2 is a good statistical indicator.

Note, however, that there is no improvement in the constraints for the parameters $\varepsilon_{\mu\alpha}^{L,R}$, since these are dominated by the CHARM II data and the restrictions from $\mu \rightarrow 3e$ for the NU and FC non-standard neutrino interactions, respectively [24].

Here a comment on FC NSI is in order. Clearly, if there are FC NSI on neutrinos one expects, by SU(2) gauge symmetry, that these will induce also FC on charged leptons, which are rather strongly constrained by the non-observation of the corresponding LFV processes such as $\mu \rightarrow e\gamma$, $\mu \rightarrow 3e$, $\mu \rightarrow e$ conversion in nuclei, $\tau \rightarrow \mu\bar{e}e$, $\tau \rightarrow \mu\rho$, etc. Indeed, given the existence of the effective NSI operators one obtains, by “dressing” with weak gauge-boson exchange, a corresponding effective NSI operator involving only charged leptons. However the loop diverges logarithmically. In this case a precise prescription must be given in order to estimate the corrections since the effective interactions are nonrenormalizable, and therefore there will be a dependence on the cutoff scale Λ at which the theory is supposed to be renormalizable [24]. While the corresponding logarithmic terms can be rigorously computed when the physics producing the NSI lies at a large scale, it is certainly not so when it lies at a relatively low scale. The latter is precisely the case which is most relevant phenomenologically, for example, schemes like the extended seesaw, broken R-parity or radiative models of neutrino mass [10, 11, 12]. In these cases there is no model-independent way to rigorously compute the magnitude of the induced NSI among charged leptons in terms of that among neutrinos.

It follows that so far NSI involving neutrinos are not strongly constrained, hence the importance of the constraints reported in Table III: in contrast with LFV constraints these are robust.

Before closing this section let us mention that constraints coming from solar [18, 19], atmospheric [21, 22, 23], and MINOS [59] data can not be directly compared with the bounds obtained here since those do not probe directly the NSI parameters but only a combination of them which effectively affects neutrino propagation in matter. For example, for the solar case, the relevant quantities, ε and ε' are two effective parameters which, for $\varepsilon_{\alpha\mu}^P \sim 0$, are related with the *vectorial* couplings by:

$$\varepsilon = -\sin\theta_{23}\varepsilon_{e\tau}^V \quad \varepsilon' = \sin^2\theta_{23}\varepsilon_{\tau\tau}^V - \varepsilon_{ee}^V, \quad (24)$$

with $\varepsilon_{\alpha\beta}^V = \varepsilon_{\alpha\beta}^L + \varepsilon_{\alpha\beta}^R$. Moreover, instead of just the NSI with electrons, one should in general take into account also the possible non-standard interactions with u and d -type quarks so that the effective NSI parameter becomes: $\varepsilon_{\alpha\beta}^P \equiv \sum_{f=u,d,e} \varepsilon_{\alpha\beta}^{fP} n_f/n_e$ (with n_f the density of fermions in the medium). This leaves substantial freedom to new NSI-induced effects.

B. Flavor-conserving non-universal NSI

Barring a theory of flavor, there is no guidance on the structure of the effective four-Fermi weak interaction. Generically new physics will lead to the violation of universality as well as the violation of leptonic flavor. In view of the relatively strong constraints on lepton flavor violating processes it is reasonable, as already mentioned, to first consider the case of purely flavor-conserving non-standard interactions, in general non-universal. In this case the only relevant parameters for our analysis are the six NU $\varepsilon_{\alpha\alpha}^{L,R}$.

LSND and neutrino reactor data have been used previously in order to constrain the NU NSI parameters [31]. It was noted that due to the nature of the elastic neutrino-electron scattering there is a fourfold ambiguity in the determination of the NSI parameters. The same happens when the analysis is performed for the non-universal parameters entering the $\nu_\mu e$ and $\bar{\nu}_\mu e$ scattering in the CHARM experiment. This fourfold ambiguity is clearly seen in the first two panels in Fig. 1. The colored regions in the first panel show the two-dimensional projections in the $\varepsilon_{ee}^L - \varepsilon_{ee}^R$ plane arising from the LSND and reactor data, while the corresponding restriction on the relevant parameters $\varepsilon_{\mu\mu}^{L,R}$ arising from the CHARM experiment is displayed in the second panel of Fig. 1. Finally, the third panel shows the projection of the constraints coming from the LEP data only on the parameters $\varepsilon_{\tau\tau}^{L,R}$. The dashed ellipses in the panels indicate the projections of the constraints following from LEP data only.

These plots clearly indicate the complementarity between the “inclusive” LEP $e^+e^- \rightarrow \nu\bar{\nu}\gamma$ data with those from reactors & LSND in constraining electron-type NSIs. Similar complementarity holds between LEP data and CHARM II data when constraining muon-type NSIs.

In the global analysis where χ_{TOT}^2 is the addition of the LEP, CHARM, LSND and reactor pieces, one clearly sees how the above fourfold ambiguities are eliminated. This is illustrated in Fig. 2 where we show the allowed regions that arise from the global χ_{TOT}^2 after taking a projection over two parameters. The shaded (colored) areas shows the 90 %, 95 %, and 99 % C.L. allowed regions (corresponding to $\Delta\chi_{\text{TOT}}^2 = \Delta\chi_{\text{min}}^2 + 4.61, 5.99, 9.21$ respectively). The constraints derived from this analysis are collected in Table IV and compared with the results discussed in the previous section. One can see that the interplay between the different experiments, namely, the combination of the LEP neutrino counting results with the remaining data, plays a crucial role in providing constraints almost as stringent as in those obtained in a one-at-a-time analysis. Needless to say the global analysis establishes the robustness of these constraints since we are allowing all the six parameters to vary.

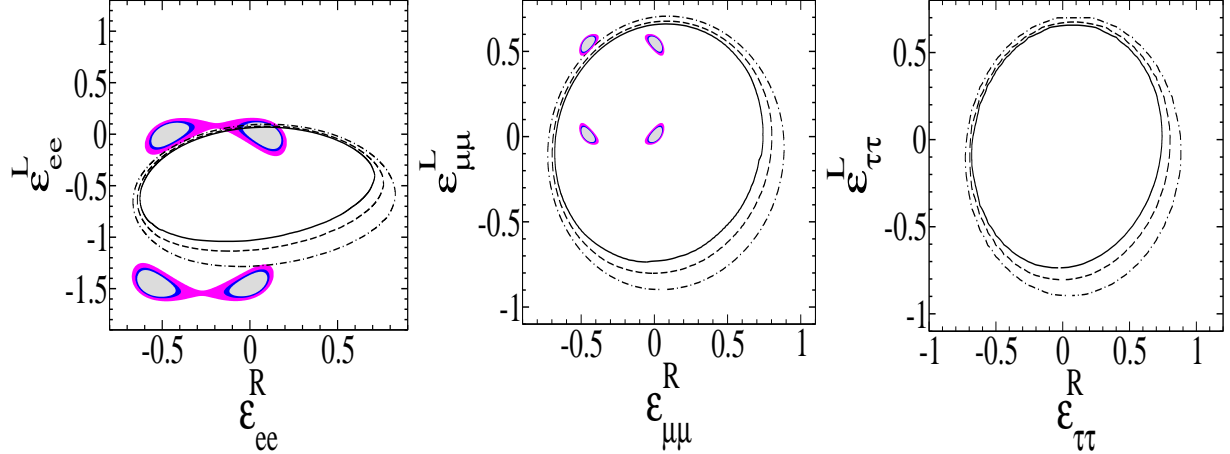


FIG. 1: Flavor conserving NSI allowed by each experiment in our analysis. The colored (shaded) regions in the first and second panel show the allowed 90 %, 95 % and 99 % C.L. regions from the $\nu_e e$ and CHARM II data, respectively. For the LEP data, we take the projection of the six free parameters, over the two displayed NSI parameters in each case. In this case, solid, dashed and dot-dashed lines show the 90 %, 95 % and 99 % CL allowed regions respectively.

TABLE IV: Constraints for the flavor conserving parameters. We have included the data from reactor, CHARM II and LEP experiments and allowed the six flavor conserving NSI to be present. The global minimum for the χ^2 analysis is $\chi^2_{min} = 23.13$, $\chi^2_{min}/\text{d.o.f.} = 1.22$. We show the 90 % C.L. values obtained after taking a projection over two parameters. For comparison, we show the constraints for the case in which only one parameter is allowed to vary, and finally, we also compare with previous reported results for the case of one parameter at a time.

	90% C.L. Allowed Region	One parameter	Previous limits
ε_{ee}^L	$-0.14 < \varepsilon_{ee}^L < 0.09$	$-0.03 < \varepsilon_{ee}^L < 0.08$	$-0.05 < \varepsilon_{ee}^L < 0.1$
ε_{ee}^R	$-0.03 < \varepsilon_{ee}^R < 0.18$	$0.004 < \varepsilon_{ee}^R < 0.15$	$0.04 < \varepsilon_{ee}^R < 0.14$
$\varepsilon_{\mu\mu}^L$	$-0.033 < \varepsilon_{\mu\mu}^L < 0.055$	$ \varepsilon_{\mu\mu}^L < 0.03$	$ \varepsilon_{\mu\mu}^L < 0.03$
$\varepsilon_{\mu\mu}^R$	$-0.040 < \varepsilon_{\mu\mu}^R < 0.053$	$ \varepsilon_{\mu\mu}^R < 0.03$	$ \varepsilon_{\mu\mu}^R < 0.03$
$\varepsilon_{\tau\tau}^L$	$-0.6 < \varepsilon_{\tau\tau}^L < 0.4$	$-0.5 < \varepsilon_{\tau\tau}^L < 0.2$	$ \varepsilon_{\tau\tau}^L < 0.5$
$\varepsilon_{\tau\tau}^R$	$-0.4 < \varepsilon_{\tau\tau}^R < 0.6$	$-0.3 < \varepsilon_{\tau\tau}^R < 0.4$	$ \varepsilon_{\tau\tau}^R < 0.5$

VI. DISCUSSION AND CONCLUSIONS

We have given a detailed analysis on non-standard neutrino interactions with electrons following from combining muon and electron (anti)-neutrino data collected in existing accel-

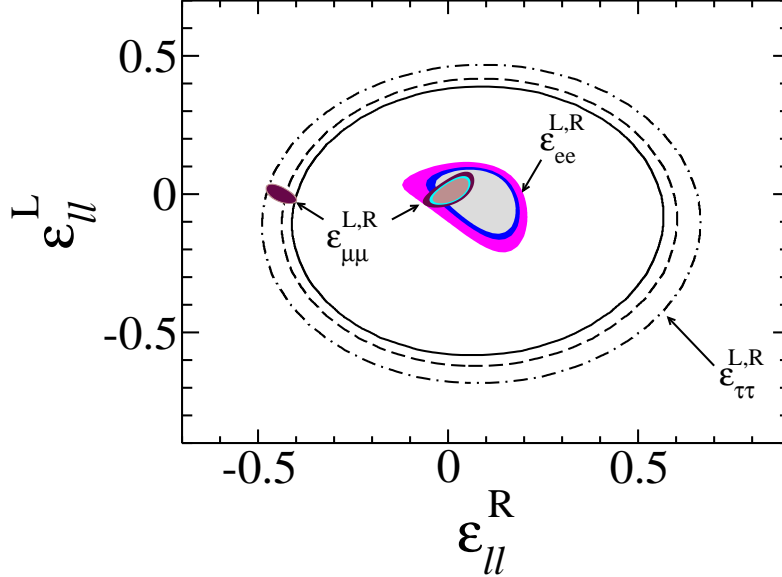


FIG. 2: Global analysis results for the flavor conserving NSI (details in Table IV). The plot shows the regions allowed at 90 %, 95 % and 99 % C.L. arising from the marginalization of the six parameters over different flavors $\epsilon_{ll}^{L,R}$, for $l = e, \mu$ and τ , as indicated. For each flavor the allowed region is unique, except for the case of $\epsilon_{\mu\mu}^{L,R}$, where there is a second solution, which is allowed only at the 99% C.L.

erators and reactors, with the high energy “neutrino counting” data from LEP. Except for $\epsilon_{\mu\mu}^{L,R}$ and most FC NSIs, the inclusion of the LEP data within a simple one-parameter-at-a-time analysis improves upon previous constraints on the flavor-conserving NSI parameters.

Barring a fundamental theory of flavor, there is no theoretical guidance on the flavor structure of the NSI that presumably result from the basic underlying theory producing neutrino masses. As a result the expected modifications in muon and electron (anti)-neutrino interactions involve the various components of the NSIs. Given this, it is necessary to perform a more general and robust analysis in which ideally all NSI parameters are allowed to vary freely. As a first step we have considered the case of non-universal NSIs. Our results indicate a strong complementarity between the “neutrino counting” data and the rest in removing the ambiguous determination of NSI parameter bounds. We have obtained unique allowed regions at 90% and 95% C.L. in NSI parameter space. Our improved constraints still leave substantial room for improvement, posing a big challenge for the next generation of neutrino experiments.

We thank Martin Hirsch and Arcadi Santamaria for useful comments. This work has been supported by CONACyT, DGAPA-UNAM, by Spanish Grant No. FPA2005-01269,

- [1] M. Maltoni, T. Schwetz, M. A. Tortola and J. W. F. Valle, *New J. Phys.* **6**, 122 (2004), Version 6 of the arXiv, hep-ph/0405172, provides updated results; previous works by other groups as well as the relevant experimental references are given therein.
- [2] G. Altarelli and F. Feruglio, *New J. Phys.* **6**, 106 (2004), [hep-ph/0405048].
- [3] P. Minkowski, *Phys. Lett.* **B67**, 421 (1977).
- [4] M. Gell-Mann, P. Ramond, and R. Slansky, *Complex Spinors and Supergravity*, in *Supergravity*, edited by P. van Nieuwenhuizen and D.Z. Freedman, North Holland, 1979.
- [5] T. Yanagida, *Horizontal gauge symmetry and masses of neutrinos*, in *Proceedings of the Workshop on the Unified Theories and the Baryon Number in the Universe*, Tsukuba, Japan, Published by KEK, 1979.
- [6] R. N. Mohapatra and G. Senjanovic, *Phys. Rev. Lett.* **44**, 912 (1980).
- [7] J. Schechter and J. W. F. Valle, *Phys. Rev.* **D22**, 2227 (1980).
- [8] J. Schechter and J. W. F. Valle, *Phys. Rev.* **D25**, 774 (1982).
- [9] R. N. Mohapatra and G. Senjanovic, *Phys. Rev.* **D23**, 165 (1981).
- [10] A. Zee, *Phys. Lett.* **B93**, 389 (1980).
- [11] K. S. Babu, *Phys. Lett.* **B203**, 132 (1988).
- [12] D. Aristizabal Sierra and M. Hirsch, *JHEP* **12**, 052 (2006), [hep-ph/0609307].
- [13] M. A. Diaz, J. C. Romao and J. W. F. Valle, *Nucl. Phys.* **B524**, 23 (1998), [hep-ph/9706315].
- [14] M. Hirsch, M.A. Diaz, W. Porod, J.C. Romao , J.W.F. Valle *Phys. Rev.* **D62**, 113008 (2000), [hep-ph/0004115], *Err-ibid.* **D65**:119901,2002.
- [15] A. Abada, S. Davidson and M. Losada, *Phys. Rev.* **D65**, 075010 (2002), [hep-ph/0111332].
- [16] M.A. Diaz, M. Hirsch, W. Porod, J.C. Romao , J.W.F. Valle *Phys. Rev.* **D68**, 013009 (2003), [hep-ph/0302021].
- [17] M. Hirsch and J. W. F. Valle, *New J. Phys.* **6**, 76 (2004), [hep-ph/0405015].
- [18] O. G. Miranda, M. A. Tortola and J. W. F. Valle, *JHEP* **10**, 008 (2006), [hep-ph/0406280].
- [19] M. M. Guzzo, P. C. de Holanda and O. L. G. Peres, *Phys. Lett.* **B591**, 1 (2004), [hep-ph/0403134].
- [20] S. Bergmann and A. Kagan, *Nucl. Phys. B* **538**, 368 (1999) [arXiv:hep-ph/9803305].
- [21] M. C. Gonzalez-Garcia *et al.*, *Phys. Rev. Lett.* **82**, 3202 (1999), [hep-ph/9809531].
- [22] A. Friedland, C. Lunardini and M. Maltoni, *Phys. Rev.* **D70**, 111301(R) (2004), [hep-ph/0408264].

- [23] N. Fornengo, M. Maltoni, R. Tomas Bayo, J. W. F. Valle Phys. Rev. **D65**, 013010 (2001), [hep-ph/0108043].
- [24] S. Davidson, C. Pena-Garay, N. Rius and A. Santamaria, JHEP **03**, 011 (2003), [hep-ph/0302093].
- [25] P. Huber, T. Schwetz and J. W. F. Valle, Phys. Rev. Lett. **88**, 101804 (2002), [hep-ph/0111224].
- [26] P. Huber, T. Schwetz and J. W. F. Valle, Phys. Rev. **D66**, 013006 (2002), [hep-ph/0202048].
- [27] J. Kopp, M. Lindner, T. Ota and J. Sato, arXiv:0710.1867 [hep-ph].
- [28] N. C. Ribeiro, H. Minakata, H. Nunokawa, S. Uchinami and R. Zukanovich-Funchal, arXiv:0709.1980 [hep-ph].
- [29] Z. Berezhiani and A. Rossi, Phys. Lett. **B535**, 207 (2002), [hep-ph/0111137].
- [30] J. Abdallah *et al.* [DELPHI Collaboration], Eur. Phys. J. C **38**, 395 (2005) [arXiv:hep-ex/0406019].
- [31] J. Barranco, O. G. Miranda, C. A. Moura and J. W. F. Valle, Phys. Rev. **D73**, 113001 (2006), [hep-ph/0512195].
- [32] ALEPH collaboration, R. Barate *et al.*, Phys. Lett. **B420**, 127 (1998), [hep-ex/9710009].
- [33] ALEPH collaboration, R. Barate *et al.*, Phys. Lett. **B429**, 201 (1998).
- [34] ALEPH collaboration, A. Heister *et al.*, Eur. Phys. J. **C28**, 1 (2003).
- [35] DELPHI collaboration, P. Abreu *et al.*, Eur. Phys. J. **C17**, 53 (2000), [hep-ex/0103044].
- [36] L3 collaboration, M. Acciarri *et al.*, Phys. Lett. **B415**, 299 (1997).
- [37] L3 collaboration, M. Acciarri *et al.*, Phys. Lett. **B444**, 503 (1998).
- [38] L3 collaboration, M. Acciarri *et al.*, Phys. Lett. **B470**, 268 (1999), [hep-ex/9910009].
- [39] OPAL collaboration, K. Ackerstaff *et al.*, Eur. Phys. J. **C2**, 607 (1998), [hep-ex/9801024].
- [40] OPAL collaboration, G. Abbiendi *et al.*, Eur. Phys. J. **C8**, 23 (1999), [hep-ex/9810021].
- [41] OPAL collaboration, G. Abbiendi *et al.*, Eur. Phys. J. **C18**, 253 (2000), [hep-ex/0005002].
- [42] M. Hirsch, E. Nardi and D. Restrepo, Phys. Rev. **D67**, 033005 (2003), [hep-ph/0210137].
- [43] LSND collaboration, L. B. Auerbach *et al.*, Phys. Rev. **D63**, 112001 (2001), [hep-ex/0101039].
- [44] F. Reines, H. S. Gurr and H. W. Sobel, Phys. Rev. Lett. **37**, 315 (1976).
- [45] MUNU collaboration, Z. Daraktchieva *et al.*, Phys. Lett. **B564**, 190 (2003), [hep-ex/0304011].
- [46] A. I. Derbin *et al.*, JETP Lett. **57**, 768 (1993).
- [47] CHARM-II collaboration, P. Vilain *et al.*, Phys. Lett. **B335**, 246 (1994).
- [48] R. N. Mohapatra and J. W. F. Valle, Phys. Rev. **D34**, 1642 (1986).
- [49] M. C. Gonzalez-Garcia and J. W. F. Valle, Phys. Lett. **B216**, 360 (1989).
- [50] J. W. F. Valle, Phys. Lett. **B199**, 432 (1987).
- [51] S. Goswami and T. Ota, arXiv:0802.1434 [hep-ph].

- [52] H. Nunokawa, Y. Z. Qian, A. Rossi and J. W. F. Valle, Phys. Rev. **D54**, 4356 (1996), [hep-ph/9605301].
- [53] A. Esteban-Pretel, R. Tomas and J. W. F. Valle, Phys. Rev. **D76**, 053001 (2007), [arXiv:0704.0032 [hep-ph]].
- [54] L. J. Hall and M. Suzuki, Nucl. Phys. **B231**, 419 (1984).
- [55] G. G. Ross and J. W. F. Valle, Phys. Lett. **B151**, 375 (1985).
- [56] A. Santamaria and J. W. F. Valle, Phys. Lett. **B195**, 423 (1987).
- [57] O. Nicrosini and L. Trentadue, Nucl. Phys. **B318**, 1 (1989).
- [58] LEP Collaborations, Phys. Lett. B **276**, 247 (1992).
- [59] A. Friedland and C. Lunardini, Phys. Rev. **D74**, 033012 (2006), [hep-ph/0606101].
- [60] F. Deppisch, T. S. Kosmas and J. W. F. Valle, Nucl. Phys. **B752**, 80 (2006), [hep-ph/0512360].
- [61] F. Deppisch and J. W. F. Valle, Phys. Rev. **D72**, 036001 (2005), [hep-ph/0406040].
- [62] M. Malinsky, J. C. Romao and J. W. F. Valle, Phys. Rev. Lett. **95**, 161801 (2005), [hep-ph/0506296].
- [63] J. Bernabeu *et al.*, Phys. Lett. **B187**, 303 (1987).
- [64] G. C. Branco, M. N. Rebelo and J. W. F. Valle, Phys. Lett. **B225**, 385 (1989).
- [65] N. Rius and J. W. F. Valle, Phys. Lett. **B246**, 249 (1990).
- [66] For supersymmetric version of the same model see Refs [60, 61]. Attempts to embed extended seesaw schemes in SO(10) lead to even more exotic varieties of seesaw, like the linear seesaw described in Ref. [62].
- [67] It also provides an explicit example for flavour and CP violation completely detached from the smallness of neutrino masses [63, 64, 65]
- [68] We have also found that different error assignment prescriptions do not substantially affect the results.